Journal of Nuclear Medicine, published on October 20, 2016 as doi:10.2967/jnumed.116.176958

Microarray Studies on ^{211}At Administration in BALB/c Nude Mice Indicate Systemic Effects on Transcriptional Regulation in Non-Thyroid Tissues

Britta Langen[1,2], Nils Rudqvist[1], Khalil Helou[3], Eva Forssell-Aronsson[1]

[1]Department of Radiation Physics, Institute of Clinical Sciences, Sahlgrenska Cancer Center, Sahlgrenska Academy, University of Gothenburg, Gothenburg, Sweden

[2]Department of Applied Physics, Chalmers University of Technology, Gothenburg, Sweden

[3]Department of Oncology, Institute of Clinical Sciences, Sahlgrenska Cancer Center, Sahlgrenska Academy, University of Gothenburg, Gothenburg, Sweden

Corresponding author / first author: Britta Langen, PhD, Department of Radiation Physics, University of Gothenburg, Sahlgrenska University Hospital, SE-413 45 Gothenburg, Sweden.

Telephone: +46-(0)31-3424023; E-mail: britta.langen@gu.se

Words: 5376

Number of tables and figures: 3 figures, 3 tables
Number of supplemental material: 4 supplemental tables, 1 supplemental information

Running title: ^{211}At-induced systemic effects in mouse

ABSTRACT

Introduction: Targeted α-therapy is a promising treatment option for various types of malignant tumors. Radiolabeled cancer-seeking agents, however, undergo degradation resulting in a certain percentage of free radionuclide in the body. The radiohalogen ^{211}At accumulates in various tissues with specifically high uptake in the thyroid. When normal thyroid function is disturbed due to ionizing radiation (IR) exposure, deleterious effects can occur in tissues that depend on thyroid hormone (TH) regulation for normal physiological function. However, knowledge of systemic effects is still rudimentary. We previously reported similarities in transcriptomic regulation between the thyroid and other tissues despite large differences in absorbed dose from ^{211}At (Langen *et al*. JNM, 2013). Here, we present supportive evidence on systemic effects after ^{211}At administration. **Methods:** Expression microarray data from kidney cortex and medulla, liver, lungs, and spleen were used from previous studies where mice were i.v. injected with 0.064–42 kBq ^{211}At and killed after 24 h, or injected with 1.7 kBq ^{211}At and killed after 1, 6, or 168 h. Controls were mock-treated and killed after 24 h. Literature-based gene signatures were used to evaluate the relative impact from IR- or TH-induced regulation. Thyroid- and TH-associated upstream regulators as well as thyroid-related diseases and functions were generated using functional analysis software. **Results:** Responses in IR- or TH-associated gene signatures were tissue-specific, varied over time, and the relative impact of each gene signature differed between the investigated tissues. The liver showed a clear dominance of TH-responding genes. In the kidney cortex, kidney medulla, and lungs, the TH-associated signature was detected to at least similar extent as the IR-associated signature. The spleen was the single tissue showing regulation of only IR-associated signature genes. Various thyroid-associated diseases and functions were inferred from the data: L-triiodothyronine, TH, TH receptor, and triiodothyronine (reverse) were inferred as upstream-regulators with differences in incidence and strength of regulation depending on tissue type. **Conclusion:** These findings indicate that transcriptional regulation in various non-thyroid tissues was–in part–induced by thyroid (hormone)-dependent signaling. Consideration of the systemic context between tissues could contribute to normal tissue risk assessment and planning of remedial measures.

Keywords: Astatine-211, radionuclide therapy, normal tissue response, systemic effects, radiogenomics

INTRODUCTION

An organism is a complex network of interdependent functional units, which can be studied on the level of interacting molecules, communicating cells in a tissue, or organs within the body. Although understood in principle, interdependencies between cells, tissues, and organs can remain elusive in experimental settings *in vivo* and pose a challenge for estimation and limitation of long-term side effects in medical practice. In radionuclide therapy, cancer-targeting agents are labeled with radionuclides and administered intravenously or locally to specifically bind to and kill malignant cells, i.e. to cause a strong and localized therapeutic effect in a systemic setting. In the 1960s and 1970s, several experiments were conducted studying systemic effects in an organism upon (localized) ionizing radiation (IR) exposure (*1–5*). This venue, however, became less prominent in the following decades when research focused on *in vitro* studies and the molecular mechanisms underlying cellular responses. In a different fashion, the systemic aspect recurred with the description of the bystander phenomenon in the 1990s (*6–9*), showing that non-hit cells within an exposed population responded to (molecular) signals from hit cells mimicking IR-induced damage and response, although the former were not subjected to ionization events. In 2005, Mothersill and colleagues discussed the systemic aspect and multi-organ involvement *in vivo*, however in a high-dose exposure setting (*10*). Knowledge of systemic effects to low-dose exposure *in vivo* is still scarce but essential, in particular for nuclear medicine. The α-emitter astatine-211 (^{211}At) is proposed for targeted radiotherapy of various malignancies, in particular metastasized tumors (*11–14*). A certain percentage of the labeled compound, however, usually degrade and accumulate in the thyroid and to a lesser degree in various other tissues (*15–20*), resulting in differential low-dose IR exposure within the body.

In previous work, we studied transcriptomic regulation profiles and individual gene regulation in response to ^{211}At, in particular after 24 h following injection of 0.064–42 kBq ^{211}At in BALB/c nude mice (*21,22*). Despite large differences in absorbed dose level between the thyroid and less accumulating tissues such as the kidneys, liver, lungs, and spleen, we observed distinct similarities in genome-wide transcriptional intensity between the thyroid and these tissues. We then hypothesized that observed responses were not exclusively induced by IR exposure in each tissue, but were in part influenced by e.g. thyroid hormones (TH) or systemic factors originating from the dominantly ^{211}At-accumulating thyroid gland (*22*). While the study design did not allow for direct evidence of thyroid-dependent

effects in non-thyroid tissues, the comprehensive microarray data can be analyzed with dedicated statistical software that can predict changes in biological functions indicative of a certain stimulus or outcome.

The aim of the present study was to determine if the observed transcriptomic regulation in non-thyroid tissues indicated systemic effects originating from the thyroid based on previous microarray data. We performed functional analysis with regard to TH regulation and pathway regulation related to thyroid disorders. Furthermore, we used signature gene analysis to assess the relative impact that IR exposure or TH-induced regulation may have on transcriptomic responses in non-thyroid tissues.

MATERIALS AND METHODS

Experimental design

This follow-up study was performed on microarray data obtained from four experimental studies discussed elsewhere (*21–24*). Briefly, ^{211}At was produced via the ^{209}Bi(a,2n)^{211}At reaction at the Cyclotron and PET Unit at Rigshospitalet in Copenhagen, Denmark, and express-delivered to Gothenburg, Sweden. Free ^{211}At was prepared via dry-distillation of the irradiated target on-site with isolation yields of 92 ± 3%, with distillation taking between 1–2 minutes as described by Lindegren *et al.* (*25*). Altogether, the procedure was performed within about 1–1.5 half-lives after irradiation of the target. The radioactivity purity was checked carefully after distillation being close to 100% in the solutions used. The solutions used in animal experiments were prepared and administered quickly afterwards, in order to ensure that ^{211}At was in the state of astatide.

Six-month-old female BALB/c nude mice (Charles River; Salzfeld, Germany) were intravenously injected with ^{211}At prepared in saline solution at various activity concentrations or mock-treated as controls (n=3/group). In the dose-range studies, responses were analyzed after 24 h following administration of 0.064, 0.64, 1.8, 14, or 42 kBq ^{211}At (*21,22*). In the short-time studies, an activity of 1.7 kBq was administered and responses studied after 1 h, 6 h, or 7 days (*23,24*). The control group was mock-treated with physiological saline and killed after 24 h. The administered activities were chosen to deliver a desired absorbed dose over a certain period to the thyroid. In the dose range study, the administered activities were chosen to cover a wide dose range from very low over moderate to very high absorbed dose to the thyroid over one day. In the time range study, a low activity was chosen to result in

(very) low absorbed dose even over one week. BALB/c nude mice were chosen since the strain is routinely used in experimental research on human tumor xenografts. The experiments were designed in the context of studying normal tissue effects in tumor-bearing mice treated with radionuclides or radiolabeled agents. Animal handling and preparation of tissue samples have been described previously (*22*). Tissue-specific absorbed dose was adapted from previously published work (*21–24*); briefly absorbed dose was calculated using the MIRD formalism (*26*). All studies were approved by the Ethical Committee on Animal Experiments in Gothenburg, Sweden.

Transcriptional analysis

Transcriptional analysis was performed on microarray data deposited in NCBI's Gene Expression Omnibus with accessions GEO:GSE32306 (*21*), GEO:GSE40806 (*22*), GEO:GSE56894 (*23*), and GEO:GSE66089 (*24*). Briefly, genome-wide transcriptional regulation was analyzed using Illumina MouseRef-8 Whole-Genome Expression BeadChips (Illumina; San Diego, CA, USA) and Nexus Expression 2.0 (BioDiscovery; El Segundo, CA, USA) as described elsewhere (*22,27*). Significantly regulated transcripts (hereafter referred to as *regulated*) were controlled for false discovery rate according to the Benjamini-Hochberg method (*28*) with an adjusted *P* value cutoff of 0.01 and a fold-change threshold of at least 1.5. Thyroid-associated upstream regulators and diseases and functions were generated using Ingenuity Pathway Analysis (IPA, Ingenuity® Systems, www.ingenuity.com; Redwood City, CA) with Fisher's exact test (*P* value <0.05).

Transcript expression signatures

In order to discern between IR- and TH-induced responses, literature-based signature genes were compiled and the microarray data (*21–24*) was analyzed with regard to significantly regulated transcripts within respective signatures. The IR-associated gene signature was composed of 56 genes adapted from Snyder and Morgan (*29*) and Chaudhry (*30*) as presented in Supplemental Table 1; the list also contains information on known RNA expression of human homologs according to the Human Protein Atlas (http://www.proteinatlas.org). For TH-associated responses, a list of 61 genes and gene groups (encoding multimeric protein) was based on literature; please refer to Supplemental Table 2 for gene list, references, and known RNA expression of human homologs. It should be noted

that various studies on TH-induced responses have been performed on the protein level without investigating the level of transcriptional regulation. In these cases, gene regulation was inferred.

RESULTS

Transcriptional regulation and absorbed dose

The dose-response studies (*21,22*) showed a distinctly similar pattern in total transcriptional regulation after 24 h for all investigated tissues (Fig. 1). A similar substantial decrease in transcript regulation was observed in all tissues between 0.64 and 1.8 kBq ^{211}At, although thyroid and non-thyroid tissues were subjected to distinctly different absorbed dose levels by a factor of ~10^2. Distinct dissimilarities between absorbed dose and number of regulated transcripts were observed between tissues. For instance, the spleen showed between 80 and 94% of the total number of transcripts regulated in the thyroid upon administration of 0.064 and 0.64 kBq ^{211}At, respectively, while receiving only around 1% of absorbed dose to thyroid. Consecutive studies (*23,24*) on transcriptional regulation over time in response to medium-activity (1.7–1.8 kBq) ^{211}At administration further indicated that the extent of transcriptional regulation was tissue-specific (Fig. 1). The liver and cortical and medullary kidney tissues received a similar absorbed dose level, but showed pronounced differences in the total number of significantly regulated transcripts; moreover, the ratio of regulated transcripts between the tissues varied over time. Interestingly, these tissues received the lowest absorbed dose levels, but showed stronger overall transcriptional responses (with the exception of kidney medulla at 7 d) than the lungs and spleen (Fig. 2). Among non-thyroid tissues, the lungs received highest absorbed dose levels, but showed similar response intensity as spleen across all time points. Dissimilarities between absorbed dose and response intensity were also observed in the time-range study. For instance, both kidney tissues received similar absorbed dose, but after 7 d, around 100 transcripts were regulated in the kidney cortex while regulation in the kidney medulla was only marginal. In contrast, liver tissue received only around 1% of absorbed dose to thyroid over 1 h, but the tissue still showed 71% of thyroid response intensity at this early time point.

Signature gene regulation

The microarray data sets were analyzed with regard to transcript up- or down-regulation of genes associated with IR or responding to TH regulation (Fig. 3). The transcriptional response for either gene signature showed tissue-

specificity, varied over time, and supported the dissimilarity between response intensity and absorbed dose level. Detailed information on regulated gene, probe ID, and fold change for respective signatures is shown in Supplemental Tables 3 and 4. The number of regulated genes for either signature ranged between 0 and 6. In kidney cortex (Fig. 3A), transcriptional responses to TH were observed at all time points, while responses to IR-associated genes were only seen after 1 and 6 h. The number of regulated TH-responding genes was higher than IR-associated genes across all time points except at 1 h, where both signatures showed regulation of 2 genes. Kidney medulla (Fig. 3B) showed a slightly increased number of regulated genes in both signatures compared with cortical tissue, however, no responses were detected for either signature after 7 d. Liver (Fig. 3C) showed a distinctly stronger response in genes associated with TH-induced regulation, which dominated over IR-associated regulation consistently across all time points. For both signatures, the regulatory incidences decreased with time and no regulation was detected in IR-associated genes after 7 d. In lung tissue (Fig. 3D), TH-responding genes were regulated after 1 h (1 gene) and after 24 h (2 genes), while IR-associated genes were regulated only after 1 h (2 genes). Spleen (Fig. 3E) showed no response in TH-responding genes at any investigated time point and exhibited regulatory responses only to IR-associated genes, i.e. after 1 h (1 gene), 24 h (2 genes), and 7 d (1 gene). Interestingly, lung tissue showed the lowest incidence in IR-associated genes, although it received highest absorbed dose among non-thyroid tissues.

Thyroid- and TH-associated pathways und regulators

Pathway analysis predicted regulation of several TH-associated upstream regulators in all tissues, but the incidence varied between tissues and time points (Table 1). The liver and kidney cortex showed the highest incidence with 3–4 and 1–3 significantly detected upstream regulators per time point, respectively. In the kidney medulla, lungs, and spleen, upstream regulators were only identified at intermittent time points. L-triiodothyronine exhibited the highest overall response in the cohort showing a trend towards activation at early time points and a trend towards inhibition after 7 d in kidney cortex and liver. L-triiodothyronine was further detected in the lungs after 24 h and in spleen after 1 h, but not in the kidney medulla. Further identified upstream regulators were TH, TH receptor, and triiodothyronine (reverse). The majority of predicted TH-associated biological functions and diseases were related to endocrine system disorders and thyroid cancer (carcinoma) (Tables 2,3). The incidence of TH-associated diseases

and functions generally showed different trends in time-response compared with upstream regulators. In the kidney cortex and liver, upstream regulators were continuously detected, while responses in disorders and functions were only identified after 6 h, or after 24 h and 7 d, respectively. Liver showed by far the highest incidence with 15 detected disorders or functions (Table 3), which was in agreement with showing the highest incidence of upstream regulators. Interestingly, detection incidence was distinctly higher in the kidney medulla and spleen compared with upstream regulators, while the lungs did not show any responses regarding diseases and functions.

DISCUSSION

Regulation of gene expression in response to a stressor is a multi-stage process. Aside from epigenetic factors and transcriptional regulation, transcript expression levels represent the first stage of gene expression which in turn regulates cellular responses. High-throughput technologies such as expression microarrays allow analysis of genome-wide transcriptional regulation without restricting the analytical frame to a limited set of genes or pathways. This approach is particularly beneficial for an *in vivo* setting with differential dose exposure, where the analytical frame must cover a multi-factorial and tissue-specific context. In case of free ^{211}At, the regulatory thyroid gland is dominantly affected by IR exposure due to specifically high uptake. Gene regulation in the thyroid gland in response to ^{211}At has been analyzed in detail in related studies (*21*,*24*). Other tissues that underlie thyroid-dependent metabolic regulation also exhibit ^{211}At uptake, but at a much lower level. (For additional information on ^{211}At characterization and considerations for biodistribution and absorbed dose, please refer to Supplemental Information S1).

Inter-organ signaling from the thyroid gland to target tissues introduces systemically induced gene regulation in addition to IR-induced gene regulation in each tissue. In theory, systemic effects originating from the thyroid gland could be caused by changes in synthesis or secretion of physiological signaling factors, i.e. TH or calcitonin, or by IR-induced long-range non-targeted signaling that would be mediated by other factors. Since knowledge of specific target genes for bystander effects is still scarce, especially in the *in vivo* context, the type or mechanism of long-range bystander signaling could not be discerned in this setup. Instead, the aim of the study was to demonstrate the regulation of TH-responding genes and thyroid-related pathway regulation in non-thyroid tissues. The systemic physiological context, however, does not exclude the possible contribution of strictly IR-associated long-range non-targeted effects in this setting. The analysis of signature gene responses in non-thyroid tissues supported the

hypothesis (*22*) that transcriptional regulation in these tissues was not solely due to IR exposure, but in part due to thyroid-dependent signaling. TH-related responses in non-thyroid tissues were also demonstrated using pathway analysis. The relative contribution to the overall transcriptional regulation, however, could not be inferred from this type of data. It should further be noted that in literature, *Ccnd1*, *Cdkn1a*, *Fos*, *Mapk1*, and *Mdm2* are associated with both IR- and TH-induced gene regulation and were used for both signatures, accordingly. It is difficult to discern if these genes were regulated in response to one or both inducers in this setting.

Irrespective of the underlying mechanisms, systemic effects appear to have a strong impact on normal tissue gene regulation, which ultimately can influence tissue health status. The available data suggest that the quality and extent of systemic effects is dependent on various physical and biological factors concerning not only the type of exposure, but also what tissue is irradiated. Clinical practice, however, does not consider systemic effects in normal tissue risk assessment. There is a need for basic research and clinical investigations to elucidate the molecular mechanisms that mediate these effects and to understand the parameters that lead to detrimental, beneficial, or insignificant systemic effects. Once these mechanisms are understood on the physical and biological levels, clinicians will be able to estimate the extent and quality of systemic effects in diagnostic and treatment planning and can give tissue-specific prophylactic countermeasures, if needed.

In general, tissue-specificity was seen regarding continuous vs. intermittent regulation, strength of regulation, and number of incidence. Although trends in activation or inhibition were observed, respective z-scores did not exceed the threshold of ±2.0 for statistical significance. The liver showed the highest incidence of response regarding both upstream regulators and identified diseases and functions, which–taken together with its strong response in signature gene analysis–indicated that it may be a major target tissue of thyroid-dependent regulation among the investigated tissues. In the kidney cortex and liver, a general time-dependent trend was observed for L-triiodothyronine (T3) with activation at early time points after ^{211}At administration and inhibition after one week. In contrast, the TH receptor as an upstream regulator was only inferred at 1 h in either tissue. TH receptors are nuclear receptors that function as transcription factors after binding to TH; hence, the functional outcome regarding transcript expression is dependent on up- or down-regulation of both hormone and receptor. Interestingly, several diseases and functions were identified in all tissues (except lungs) that were not only related to TH, but also to thyroid tissue-specific disorders and processes. These identified pathways could comprise target genes of normal TH-dependent regulation that are

associated with thyroid-specific diseases in the database, but are not biologically related to disorders in non-thyroid tissues. It is also possible that these responses indicate non-targeted effects that are reminiscent of IR-induced effects in thyroid tissue.

Another unknown factor is tissue-specific response over time, as tissues are categorized as early or late responding with regard to IR-induced responses (*31*). As such, responses in a tissue may be best related to the tissue-specific *time of on-set* and not to a certain time point after administration. This might also be valid for TH-induced responses, but to the best of our knowledge, the temporal context of this systemic regulation has not been established on the transcriptional level in the target tissues of interest.

CONCLUSION

This consecutive study on transcriptomic regulation following intravenous ^{211}At administration supported the previously postulated hypothesis that transcriptional responses in the liver, lungs, spleen, and kidney tissues are influenced–in part–by thyroid-dependent effects. Although it was not possible to demonstrate direct causality in the given setup, TH-associated signature genes were regulated more frequently than IR-associated signature genes. The strength of response for either signature appeared to be tissue-specific. Furthermore, upstream regulators related to TH and diseases and functions related to thyroid (hormones) were detected in non-thyroid tissues using Ingenuity Pathway Analysis; moreover, tissue-specific variation in response intensity as well as time-of-response were also observed. These findings demonstrate the complexity of *in vivo* responses and the need to consider organs in a systemic context when studying normal tissue responses to systemically administered radionuclides.

ACKNOWLEDGEMENTS

The authors thank the following organizations for financial support of this study: the European Commission FP7 Collaborative Project TARCC HEALTH-F2-2007-201962, the Swedish Research Council (grant no. 21073), the Swedish Cancer Society (grant no. 3427), BioCARE – a National Strategic Research Program at the University of Gothenburg, the Swedish Radiation Safety Authority, the King Gustav V Jubilee Clinic Cancer Research

Foundation, the Sahlgrenska University Hospital Research Funds, the Assar Gabrielsson Cancer Research Foundation, the Adlerbertska Research Fund, and the Wilhelm och Martina Lundgren science trust fund.

REFERENCES

1. Ackerman JL, Linsk JA, Shuman BJ. The systemic effects of localized radiation on serum proteins in humans. A preliminary report. *Am J Roentgenol Radium Ther Nucl Med.* 1962;87:543–546.
2. Skoog WA, Adams WS. Multiple myeloma with a large extramedullary plasmacytoma of the thorax treated with prednisone and radiation metabolic balance study demonstrating unusual beneficial systemic effects of radiation ablation of the plasmacytoma. *Stanford Med Bull.* 1962;20:87–101.
3. Phillips RD, Kimeldorf DJ. An analysis of local and systemic effects of ionizing radiation on bone growth. USNRDL-TR-898. *Res Dev Tech Rep.* 1965;25:1–21.
4. Phillips RD, Kimeldorf DJ. Local and systemic effects of ionizing radiation on bone growth. *Am J Physiol.* 1966;210:1096–1100.
5. Yuile CL, Gibb FR, Morrow PE. Dose-related local and systemic effects of inhaled plutonium-238 and plutonium-239 dioxide in dogs. *Radiat Res.* 1970;44:821–834.
6. Nagasawa H, Little JB. Induction of sister chromatid exchanges by extremely low doses of alpha-particles. *Cancer Res.* 1992;52:6394–6396.
7. Seymour CB, Mothersill C. Delayed expression of lethal mutations and genomic instability in the progeny of human epithelial cells that survived in a bystander-killing environment. *Radiat Oncol Investig.* 1997;5:106–110.
8. Mothersill C, Seymour CB. Cell-cell contact during gamma irradiation is not required to induce a bystander effect in normal human keratinocytes: evidence for release during irradiation of a signal controlling survival into the medium. *Radiat Res.* 1998;149:256–262.
9. Nagasawa H, Little JB. Unexpected sensitivity to the induction of mutations by very low doses of alpha-particle radiation: evidence for a bystander effect. *Radiat Res.* 1999;152:552–557.
10. Mothersill C, Moriarty MJ, Seymour CB. Bystander and other delayed effects and multi-organ involvement and failure following high dose exposure to ionising radiation. *BJR Suppl.* 2005;27:128–131.
11. Harrison A. The application of ^{211}At in experimental tumor therapy. *Radiochem Acta.* 1989;47:157–161.
12. Larsen RH, Akabani G, Welsh P, Zalutsky MR. The cytotoxicity and microdosimetry of astatine-211-labeled chimeric monoclonal antibodies in human glioma and melanoma cells in vitro. *Radiat Res.* 1998;149:155–162.

13. Andersson H, Cederkrantz E, Bäck T, et al. Intraperitoneal alpha-particle radioimmunotherapy of ovarian cancer patients: pharmacokinetics and dosimetry of ^{211}At-MX35 F(ab9)2–a phase I study. *J Nucl Med.* 2009;50:1153–1160.
14. Andersson H, Lindegren S, Back T, Jacobsson L, Leser G, Horvath G. The curative and palliative potential of the monoclonal antibody MOv18 labelled with ^{211}At in nude mice with intraperitoneally growing ovarian cancer xenografts–a long-term study. *Acta Oncol.* 2000;39:741–745.
15. Hamilton JG, Durbin PW, Parrott M. The accumulation and destructive action of astatine-211 (eka-iodine) in the thyroid gland of rats and monkeys. *J Clin Endocrinol Metab.* 1954;14:1161–1178.
16. Hamilton JG, Durbin PW, Parrott MW. Accumulation of astatine-211 by thyroid gland in man. *Proc Soc Exp Biol Med.* 1954;86:366–369.
17. Brown I. Astatine-211: its possible applications in cancer therapy. *Int J Rad Appl Instrum [A].* 1986;37:789–798.
18. Lindencrona U, Nilsson M, Forssell-Aronsson E. Similarities and differences between free ^{211}At and ^{125}I-transport in porcine thyroid epithelial cells cultured in bicameral chambers. *Nucl Med Biol.* 2001;28:41–50.
19. Lundh C, Lindencrona U, Postgård P, Carlsson T, Nilsson M, Forssell-Aronsson E. Radiation-induced thyroid stunning: differential effects of ^{123}I, ^{131}I, ^{99m}Tc, and ^{211}At on iodide transport and NIS mRNA expression in cultured thyroid cells. *J Nucl Med.* 2009;50:1161–1167.
20. Garg PK, Harrison CL, Zalutsky MR. Comparative tissue distribution in mice of the alpha-emitter ^{211}At and ^{131}I as labels of a monoclonal antibody and F(ab')2 fragment. *Cancer Res.* 1990;50:3514–3520.
21. Rudqvist N, Parris TZ, Schüler E, Helou K, Forssell-Aronsson E. Transcriptional response of BALB/c mouse thyroids following in vivo astatine-211 exposure reveals distinct gene expression profiles. *EJNMMI Res.* 2012;2(1):32.
22. Langen B, Rudqvist N, Parris TZ, Schüler E, Helou K, Forssell-Aronsson E. Comparative analysis of transcriptional gene regulation indicates similar physiologic response in mouse tissues at low absorbed doses from intravenously administered ^{211}At. *J Nucl Med*. 2013;54:990–998.
23. Langen B, Rudqvist N, Parris TZ, et al. Transcriptional response in normal mouse tissues after i.v. ^{211}At administration – response related to absorbed dose, dose-rate and time. *EJNMMI Res*. 2015;5:1.

24. Rudqvist N, Spetz J, Schüler E, et al. Transcriptional response in mouse thyroid tissue after ^{211}At administration: effects of absorbed dose, initial dose-rate and time after administration. *PLoS One*. 2015;10(7):e0131686.
25. Lindegren S, Back T, Jensen HJ. Dry-distillation of astatine-211 from irradiated bismuth targets: a time saving procedure with high recovery yields. *Appl Radiat Isot.* 2001;55:157–160.
26. Bolch WE, Eckerman KF, Sgouros G, Thomas SR. MIRD pamphlet No. 21: a generalized schema for radiopharmaceutical dosimetry--standardization of nomenclature. *J Nucl Med.* 2009;50:477–484.
27. Parris TZ, Danielsson A, Nemes S, et al. Clinical implications of gene dosage and gene expression patterns in diploid breast carcinoma. *Clin Cancer Res.* 2010;16:3860–3874.
28. Benjamini Y, and Hochberg Y. Controlling the false discovery rate: a practical and powerful approach to multiple testing. *J R Statist Soc B.* 1995;57:289–300.
29. Snyder AR, and Morgan WF. Gene expression profiling after irradiation: clues to understanding acute and persistent responses? *Cancer Metastasis Rev.* 2004;23:259–268.
30. Chaudhry MA. Biomarkers for human radiation exposure. *J Biomed Sci*. 2008;15:557–563.
31. Willers H1, Held KD. Introduction to clinical radiation biology. *Hematol Oncol Clin North Am*. 2006;20(1):1–24. Review.

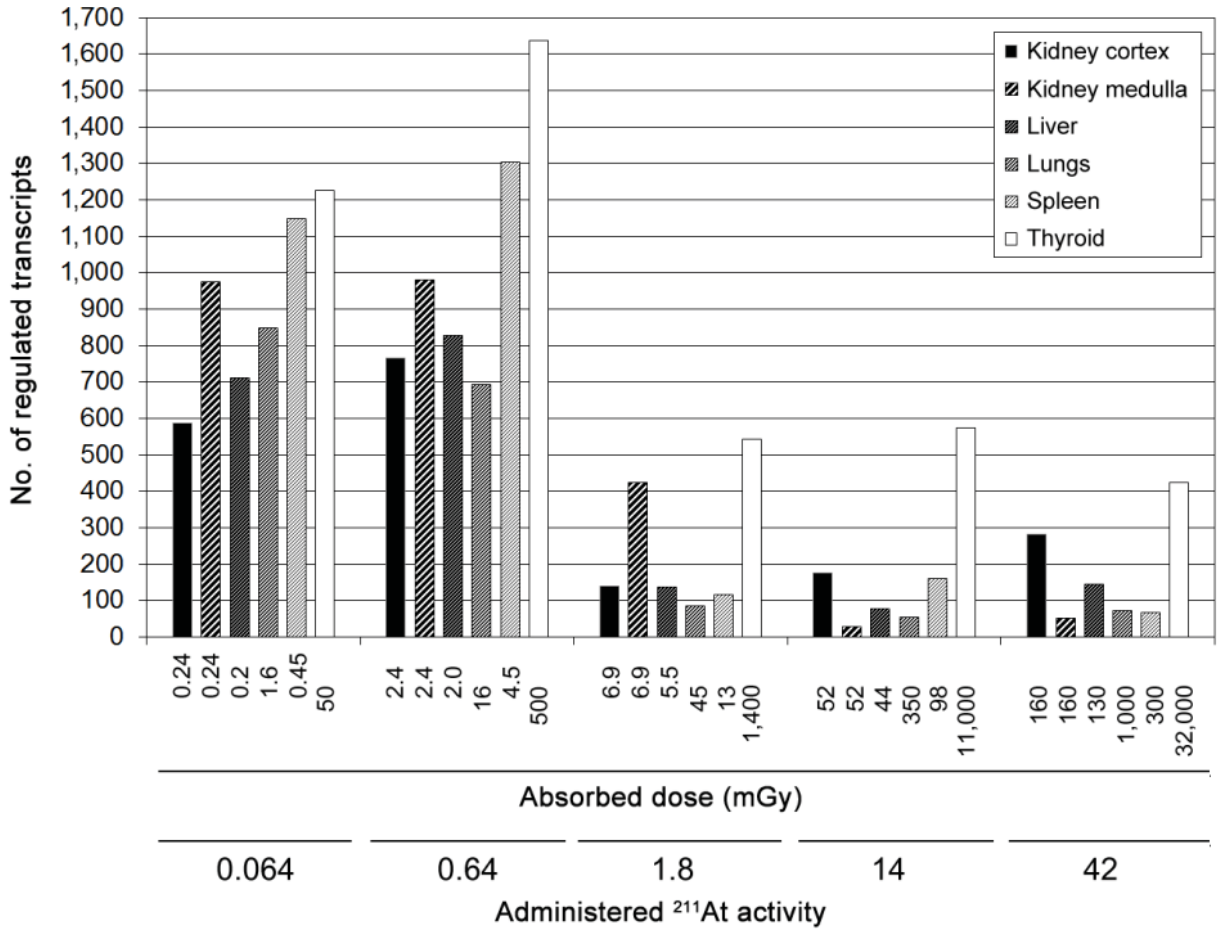

FIGURE 1. Absorbed dose and total transcript regulation after 24 h over ^{211}At activity range. Tissue-specific absorbed dose (mGy) from i.v. administered 0.064–42 kBq ^{211}At was adapted from previously presented studies on the kidney cortex and medulla, liver, lungs, and spleen (*22*), and thyroid (*21*). The number of significantly regulated transcripts includes both up- and down-regulated transcripts at a given exposure.

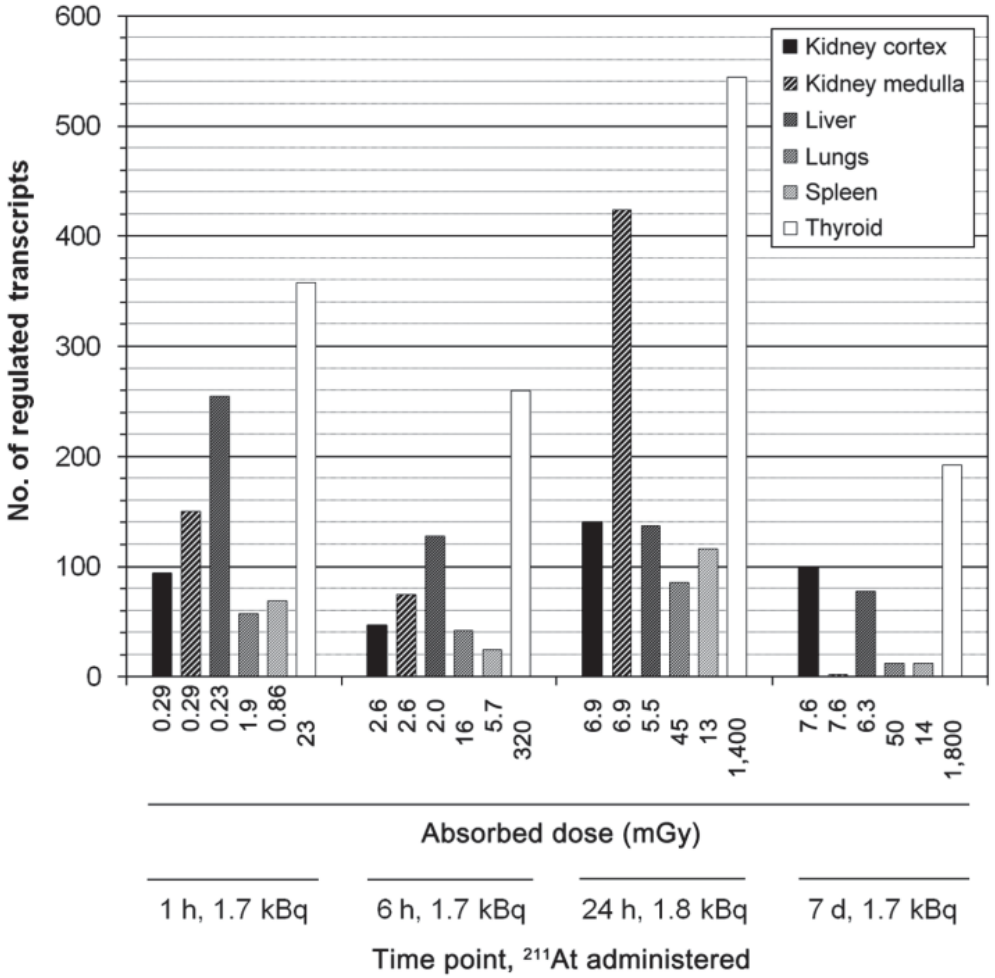

FIGURE 2. Absorbed dose and total transcript regulation over time to low ^{211}At activity. Tissue-specific absorbed dose (mGy) from i.v. administered 1.7–1.8 kBq ^{211}At was adapted from previous studies on the kidney cortex and medulla, liver, lungs, and spleen (*23*), and thyroid (*24*). The number of significantly regulated transcripts includes both up- and down-regulated transcripts at a given exposure and time point.

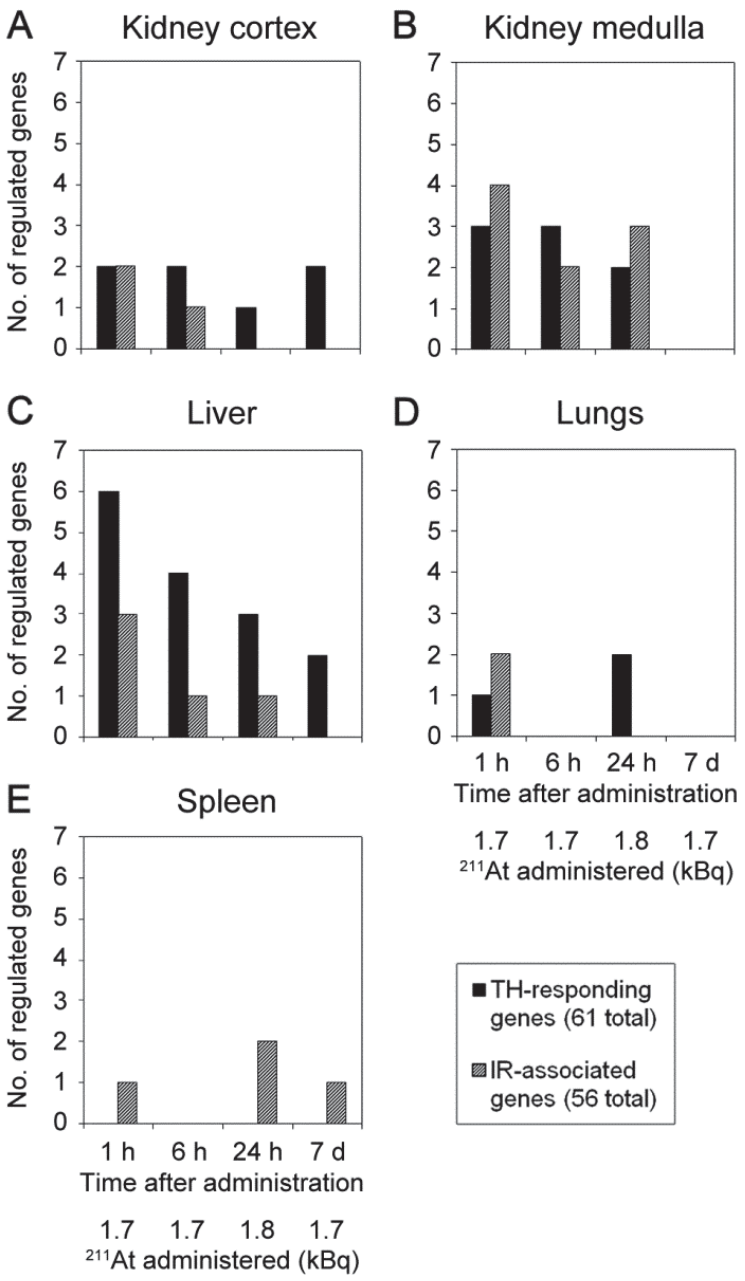

FIGURE 3. Comparison of signature gene regulation in kidney cortex and medulla, liver, lungs, and spleen. The number (no.) of significantly regulated genes at various time points after low activity ^{211}At administration is shown for genes associated with regulation induced by IR (hashed) and TH (black). Responses are shown for the kidney cortex (A), kidney medulla (B), liver (C), lungs (D), and spleen (E). Analyses were performed on microarray data GEO:GSE40806 and GEO:GSE56894 first reported in Langen *et al.,* 2013 (*22*), and Langen *et al.,* 2015 (*23*), respectively. Please refer to Supplemental Tables 3 and 4 for regulated genes, transcript identification number, and fold change values of IR-associated and TH-responding signature genes, respectively.

TABLE 1. Thyroid hormone-associated upstream regulators in non-thyroid tissues.

Tissue	Time point	Upstream regulators	Activation z-score	*P* value of overlap	Target molecules in dataset
Kidney cortex	1 h	TH	N/A	5.5E-05	AK4,G6PC,ME1,PCK1,PER1,UCP1
		L-triiodothyronine	1.7	1.5E-04	G6PC,IGFBP4,Mup1 (includes others),COA4, PCK1,UCP1
		TH receptor	N/A	4.1E-02	UCP1
	6 h	TH	N/A	5.0E-04	ACSL5,G6PC,PCK1,PER1
		L-triiodothyronine	1.2	9.7E-04	G6PC,HBA1/HBA2,PCK1,PDK4
	24 h	L-triiodothyronine	1.4	2.7E-05	ACTB,ADIPOQ,ATP2A2,C4A/C4B,FGA,Kap, LYZ,SCD
		TH	-0.15	3.4E-03	Apoc1,APOE,ATP2A2,Cdkn1c,Tmsb4x (includes others)
		triiodothyronine, reverse	N/A	2.1E-02	EGR1
	7 d	L-triiodothyronine	-0.48	1.2E-09	ADIPOQ,C4A/C4B,G6PC,HP,Kap,Mup1 (includes others),PYGL,SCD,TF,THRSP,UCP1
Kidney medulla	1 h	ND			
	6 h	ND			
	24 h	ND			
	7 d	TH	N/A	9.0E-03	Apoc1
Liver	1 h	L-triiodothyronine	1.1	1.0E-09	ABCD2,ACTB,ALB,APOA5,ATP2A2,C1S,CY P17A1,CYP7A1,G6PC,IGFBP1,LYZ,Mup1 (includes others),PCK1,POR,RGN,THRSP
		TH	1.1	3.2E-06	ATP2A2,Cyp4a14,CYP7A1,DDC,G6PC,HSP9 ,AB1,LPL, PCK1,PER1,PML,THRSP
		TH receptor	N/A	5.9E-03	ABCD2,POR
		triiodothyronine, reverse	N/A	3.9E-02	EGR1
	6 h	L-triiodothyronine	1.3	1.4E-06	ADIPOQ,CYP17A1,CYP7A1,G6PC,IGFBP1, Mup1 (includes others),PCK1,POR,THRSP
		TH	N/A	3.6E-06	ALDOB,Cyp4a14,CYP7A1,DDC,G6PC,PCK1, PER1,THRSP
		triiodothyronine, reverse	N/A	1.9E-02	EGR1
	24 h	L-triiodothyronine	-0.56	3.3E-05	DIO1,ENPP2,FGF21,HP,IGFBP1,Mup1 (includes others),SREBF1,THRSP
		TH	N/A	3.8E-03	IGFBP2,LPL,NTRK2,NUDT7,THRSP
		triiodothyronine, reverse	N/A	2.1E-02	EGR1
	7 d	L-triiodothyronine	-1.0	2.7E-08	ACTB,ALB,CYP17A1,CYP4A11,CYP7A1,DIO 1,G6PC,LYZ,Mup1 (includes others)
		TH	N/A	2.7E-03	Cyp4a14,CYP7A1,G6PC,PER1
		triiodothyronine, reverse	N/A	1.2E-02	EGR1
Lungs	1 h	triiodothyronine, reverse	N/A	9.8E-03	EGR1
	6 h	ND			
	24 h	TH	N/A	7.7E-03	LPL,ME1,MYH6,THRSP
		L-triiodothyronine	0.042	1.4E-02	ACTB,ADIPOQ,MYH6,THRSP
		triiodothyronine, reverse	N/A	1.6E-02	EGR1
	7 d	ND			
Spleen	1 h	L-triiodothyronine	N/A	2.7E-02	HP,PDK4,PYGL
	6 h	ND			
	24 h	ND			
	7 d	ND			

Upstream regulators were generated with Ingenuity Pathways Analysis (IPA) software; analysis was performed using NEXUS Expression output files of significantly regulated transcripts in response to 1.7–1.8 kBq ^{211}At at respective time points. N/A, not available; ND, not detected

TABLE 2. Thyroid-associated diseases & functions in kidneys, lungs, and spleen.

Tissue	Time point	Diseases and Functions	Annotation	*P* value	Molecules
Kidney cortex	1h	ND			
	6h	Endocrine System Disorders	familial primary hyperparathyroidism	1.1E-02	CYP24A1
		Cancer, Endocrine System Disorders	parathyroid cancer	1.9E-02	CYP24A1
		Endocrine System Disorders	secondary hyperparathyroidism	2.7E-02	CYP24A1
	24h	ND			
	7d	ND			
Kidney medulla	1 h	ND			
	6 h	ND			
	24 h	Cancer, Endocrine System Disorders	thyroid cancer	3.5E-04	ABCC3,LGALS3,NCOA4,PRLR,RB1,SLPI,SOCS3,SPHK1,SPP1,STAT3,TIMP1,TIMP3
		Cancer, Endocrine System Disorders	papillary thyroid cancer	5.0E-04	ABCC3,LGALS3,NCOA4,SPHK1,SPP1,TIMP1,TIMP3
		Cancer, Endocrine System Disorders	epithelial thyroid cancer	6.5E-04	ABCC3,LGALS3,NCOA4,PRLR,RB1,SPHK1,SPP1,STAT3,TIMP1,TIMP3
		Endocrine System Development and Function, Organ Development	activation of thyroid gland	9.3E-04	GHR,HPN,PRF1
	7 d	ND			
Lungs	1 h	ND			
	6 h	ND			
	24 h	ND			
	7 d	ND			
Spleen	1 h	Cancer, Endocrine System Disorders	incidence of medullary thyroid carcinoma	3.8E-03	PRLR
	6 h	Endocrine System Disorders, Immunological Disease, Inflammatory Disease	Hashimoto's thyroiditis	5.8E-05	CD83,CTLA4
		Endocrine System Disorders, Immunological Disease, Inflammatory Disease	susceptibility to Hashimoto's thyroiditis	3.0E-03	CTLA4
	24 h	Cell Morphology, Endocrine System Development and Function, Organ Morphology, Organismal Development	abnormal morphology of thyroid follicle cells	2.5E-02	CTSK
	7 d	ND			

Pathways were generated with Ingenuity Pathway Analysis (IPA) software; analysis was performed using NEXUS Expression output files of significantly regulated transcripts in response to 1.7–1.8 kBq ^{211}At at respective time points. ND, not detected

TABLE 3. Thyroid-associated diseases & functions in liver.

Tissue	Time point	Diseases and Functions	Annotation	*P* value	Molecules
Liver	1 h	ND			
	6 h	ND			
	24 h	Cancer, Endocrine System Disorders	asymptomatic stage medullary thyroid carcinoma	2.9E-03	EGFR,NTRK2
		Cancer, Endocrine System Disorders	locoregional medullary thyroid carcinoma	2.9E-03	EGFR,NTRK2
		Cancer, Endocrine System Disorders	metastatic medullary thyroid carcinoma	2.9E-03	EGFR,NTRK2
		Cancer, Endocrine System Disorders	progressive medullary thyroid cancer	2.9E-03	EGFR,NTRK2
	7 d	Endocrine System Disorders	benign thyroid disease	3.0E-03	ALB,DIO1,GC
		Developmental Disorder, Endocrine System Disorders, Hereditary Disorder, Metabolic Disease	dysalbuminemic hyperthyroxinemia	4.0E-03	ALB
		Endocrine System Disorders, Metabolic Disease	hyperthyroidism	6.1E-03	DIO1,GC
		Amino Acid Metabolism, Molecular Transport, Small Molecule Biochemistry	transport of L-triiodothyronine	8.1E-03	Slco1a4
		Amino Acid Metabolism, Drug Metabolism, Molecular Transport, Small Molecule Biochemistry	transport of levothyroxine	1.2E-02	Slco1a4
		Amino Acid Metabolism, Molecular Transport, Small Molecule Biochemistry	efflux of L-triiodothyronine	1.6E-02	ALB
		Amino Acid Metabolism, Drug Metabolism, Molecular Transport, Small Molecule Biochemistry	efflux of levothyroxine	1.6E-02	ALB
		Small Molecule Biochemistry	inactivation of TH	1.6E-02	DIO1
		Endocrine System Development and Function, Organ Development	activation of parathyroid gland	2.0E-02	GC
		Endocrine System Development and Function, Small Molecule Biochemistry	metabolism of TH	2.8E-02	DIO1
		Organ Development	function of thyroid gland	3.2E-02	DIO1

Pathways related to TH-associated diseases and functions were generated with Ingenuity Pathway Analysis (IPA) software; analysis was performed using NEXUS Expression output files of significantly regulated transcripts in response to 1.7–1.8 kBq ^{211}At at respective time points. ND, not detected

Supplemental Information S1.
^{211}At characterization and considerations for biodistribution and absorbed dose

It is established knowledge that ^{211}At can take different chemical states in aqueous solution. $^{211}At^-$ is taken up into the thyroid, most likely via NIS. Our earlier studies indicate, however, that ^{211}At can be taken up through other mechanisms which can also apply to other chemical states (Lindencrona *et al*., 2001). At first, ^{211}At in aqueous solution is in $^{211}At^-$ state, but over time, other chemical states are formed. This is why we handled ^{211}At in non-polar phase upon extraction and transferred it to aqueous solution only right before injection, i.e. in order to ensure that ^{211}At was in $^{211}At^-$ state as much as possible. We have followed this protocol in all of our studies with ^{211}At. Nevertheless, it is possible that the distribution among different chemical states may vary between experiments leading to somewhat different biodistribution and absorbed dose. However, the dose relation between groups within an experiment would remain the same. For small tissues such as the thyroid, it should be noted that it is not possible to measure activity concentration at the same time as sampling enough tissue for microarray analysis. Therefore, absorbed dose had to be estimated based on separately acquired biodistribution data.

SUPPLEMENTAL TABLE 1. List of ionizing radiation-associated genes

Gene symbol (*Mus musculus*)	Synonym(s)	Known RNA expression of human homolog*				
		Kidney	Liver	Lungs	Spleen	Thyroid
		Expression (FPKM)				
Amy2a5	*Amy2, Amy-2*	15	9	18	19	17
Apaf1	*Apaf1l*	5	4	7	10	5
Bag1	*Rap46*	84	31	52	38	54
Batf3		1	1	4	10	1
Bax		39	27	51	77	26
Birc2	*Api1, cIAP1, HIAP1, IAP1, MIAP1, MIHB*	24	27	23	25	23
Birc3	*Api2, cIAP2, HIAP2, IAP2, MIAP2, MIHC, RNF49*	6	19	16	58	3
Ccnb1	*Ccnb1-rs13, Cycb-4*	4	3	5	8	10
Ccnd1	*bcl-1, cD1, CycD1*	36	91	72	37	51
Ccne1	*CycE1*	1	1	1	2	2
Ccng1		101	73	37	36	74
Cdc25c	*Cdc25*	0	1	0	0	0
Cdkn1a	*CAP20, CDKI, P21*	18	58	36	11	44
Akr1c21		26	116	13	1	4
Ddb2	*p48*	5	16	14	13	6
Ephx2	*Eph2, sEH, sEP*	139	132	14	14	25
Fen1		5	6	5	8	5
Fhl2	*SLIM3*	18	15	8	13	21
Flt3	*CD135, Flk2, wmfl*	2	0	1	8	0
Fos	*cFos, D12Rfj1*	288	223	444	153	676
Gadd45a	*Ddit1*	68	116	14	10	47
Gadd45g	*CR6, OIG37*	8	36	5	1	3
Gja1	*Cx43*	14	8	63	3	144
Gjb2	*Cx26*	8	28	1	0	2
Irf8	*ICSBP, Icsbp1, IRF-8, Myls*	5	14	21	113	3
Jun	*c-jun, Junc*	80	127	72	78	132
Mapk8ip1	*IB1, Jip1, MAPK8IP1, mjip-2a, Prkm8ip, Skip*	6	2	2	1	3
Mapk1	*Erk2, MAPK2, p42mapk, Prkm1*	40	23	38	40	42
Mapk3	*Erk1, Esrk1, Mtap2k, p44erk1, p44mapk, Prkm3*	47	12	81	52	70
Mdm2		12	30	18	18	21
Mycbp	*Amy-1*	19	8	15	12	18
Naa35	*Mak10*	11	5	8	7	16
Pmaip1	*Noxa*	1	1	2	5	3
Ogg1	*Mmh*	32	7	11	13	11
Pcna		40	31	35	40	40
Plcg2		25	13	12	47	10
Rad23b	*mHR23B*	54	120	50	43	66
Rad51b	*mREC2, R51H2, Rad51l1*	6	2	5	4	12
Rhoa	*Arha, Arha1, Arha2, RhoA*	204	128	346	257	280
Rhoh	*Arhh*	1	2	4	36	1
Tgfb3		4	7	13	5	7
Tgfbr2	*TbetaRII, TBR-II*	77	33	152	104	62

Tnfaip8	*Gg2-1, Gm10539, Nded, Ssc-2*	11	6	16	57	23
Tnfrsf10b	*DR5, KILLER, TRAILR2, TRICK2A, TRICK2B, TRICKB*	15	28	27	25	25
Tnfrsf19	*TAJ, TAJ-ALPHA, TRADE, Troy*	15	0	19	5	3
Tnfrsf21	*DR6, TR7*	39	6	13	15	5
Trp53	*p53*	12	9	15	28	17
Trp53inp1	*SIP, Teap*	10	43	21	29	8
Trp53inp2	*Tp53inp2*	22	27	13	5	18
Vegfb	*Vrf*	62	20	54	44	50
Wee1		12	33	13	9	34
Xab2		18	7	17	26	18
Xiap	*Aipa, Api3, Birc4, IAP3, ILP-1*	15	9	11	11	18
Xpc		27	15	22	23	28
Xrcc1		16	7	19	19	25
Xrcc6	*Ku70, G22p1*	85	63	72	71	83

*according to Human Protein Atlas (http://www.proteinatlas.org; retrieved 2014-08-14)
FPKM, fragments per kilobase of exon per million fragments mapped

The table has been adapted from:

Langen B. (2015). Systemic effects after ionizing radiation exposure: Genome-wide transcriptional analysis of mouse normal tissues exposed to ^{211}At, ^{131}I, or 4 MV photon beam (Doctoral dissertation). Chalmers University of Technology, Gothenburg, Sweden (ISBN 978-91-7597-194-0).

The list is composed of data presented in:

Snyder AR, Morgan WF. Gene expression profiling after irradiation: clues to understanding acute and persistent responses? *Cancer Metastasis Rev.* 2004;23:259–268.

Chaudhry MA. Biomarkers for human radiation exposure. *J Biomed Sci*. 2008;15:557–563.

SUPPLEMENTAL TABLE 2. List of thyroid hormone-responding genes

Gene symbol (*Mus musculus*)	Synonym(s), comment	Reference	Known RNA expression of human homolog*				
			Kidney	Liver	Lungs	Spleen	Thyroid
			Expression (FPKM)				
Alpl	*Akp2, TNAP*	Moeller *et al.* (2011)	55	29	51	12	3
Akt1†	*Akt, PKB*	Cordeiro *et al.* (2013)	41	39	77	70	55
Angptl3	*hypl*	Moeller *et al.* (2011)	45	313	0	0	0
Atp2a1†	*SERCA1*	Kim (2008)	1	0	1	1	0
Atp5c1		Pihlajamäki *et al.* (2009)	250	146	89	92	157
Camkk1†		Cordeiro *et al.* (2013)	2	1	4	5	7
Camkk2†		Cordeiro *et al.* (2013)	15	8	20	28	13
Ccnd1	*bcl-1, cD1, CycD1*	Puzianowska-Kuznicka *et al.* (2006)	36	91	72	37	51
Cd44	*Ly-24, HERMES, Pgp-1*	Dong *et al.* (2009)	17	21	184	72	84
Cdkn1a	*CAP20, CDKI, P21*	Puzianowska-Kuznicka *et al.* (2006)	18	58	36	11	44
Cox7c	*Cox7c1, COXVIIc*	Pihlajamäki *et al.* (2009)	389	235	173	187	279
Cyp7a1†		Cordeiro *et al.* (2013)	0	17	0	0	0
E2f1		Puzianowska-Kuznicka *et al.* (2006)	0	1	3	2	1
Egf		Puzianowska-Kuznicka *et al.* (2006)	95	0	1	0	4
Egfr		Puzianowska-Kuznicka *et al.* (2006)	11	22	16	5	23
Epas1	*bHLHe73, HIF2A, HLF, HRF*	Moeller *et al.* (2011)	97	82	432	82	146
Fas†	*APO-1, CD95, TNFR6, Tnfrsf6*	Cordeiro *et al.* (2013)	9	24	24	16	10
Fgf2	*bFGF, Fgf-2, Fgfb*	Moeller *et al.* (2011)	4	1	5	1	2
Fos	*cFos, D12Rfj1*	Puzianowska-Kuznicka *et al.* (2006)	288	223	444	153	676
Fosb		Puzianowska-Kuznicka *et al.* (2006)	30	93	44	19	179
Furin	*Fur, PACE, Pcsk3, SPC1*	Moeller *et al.* (2011)	25	66	32	26	40
G6pc	*G6Pase, G6pt*	Lin *et al.* (2013)	54	136	0	0	0
Gsta1	(human homolog *GSTA1* as representative of RNA expression in tissue	Lin *et al.* (2013)	739	1020	14	0	0
Gtf3c1		Dong *et al.* (2009)	18	9	17	16	33
Hadha†	*Mtpa*	Chocron *et al.* (2012)	97	97	51	52	66
Hif1a	*bHLHe78, MOP1*	Lin *et al.* (2013); Moeller *et al.* (2011)	70	35	40	65	55
Hnrnph3	*hnRNP, 2H9, Hnrph3*	Pihlajamäki *et al.* (2009)	94	56	98	112	123
Ifi27	*Ifi27l1*	Puzianowska-Kuznicka *et al.* (2006)	73	39	388	480	52
Ldlr†		Cordeiro *et al.* (2013)	6	62	52	11	3
Lmo2	*Rbtn2, Rhom2*	Dong *et al.* (2009)	31	7	35	35	12
Mag	*Gma, siglec-4a*	Dong *et al.* (2009)	1	1	1	0	1
Mapk1†	*Erk2, MAPK2, Prkm1*	Cordeiro *et al.* (2013)	40	23	38	40	42
Mbp	*golli-mbp, Hmbpr*	Dong *et al.* (2009)	21	12	22	26	26
Mcl1		Moeller *et al.* (2011)	95	262	162	174	168
Mdm2		Puzianowska-Kuznicka *et al.* (2006)	12	30	18	18	21
Myh6	*alpha-MHC, alpha myosin, Myhca*	Moeller *et al.* (2011)	0	0	0	0	0
Ncor1†	*N-CoR, mKIAA1047,*	Söderström *et al.* (1997);	34	57	28	34	40

	Rxrip13	Cheng *et al.* (2010)					
Ncor2†	*SMRT*	Söderström *et al.* (1997); Cheng *et al.* (2010)	22	9	40	34	18
Nos1†	*bNOS, nNOS, NO, Nos-1*	Carreras *et al.* (2001)	2	0	1	0	0
Pck1	*PEPCK*	Lin *et al.* (2013)	490	687	0	0	0
Pfkp	*PFK-C*	Moeller *et al.* (2011)	33	3	13	21	33
Pik3ca†	*caPI3K, p110alpha*	Cordeiro *et al.* (2013)	11	7	12	13	11
Prka† *family*	human homolog *PRKAA1* as representative of RNA expression in tissue	Cordeiro *et al.* (2013)	35	34	36	35	43
Prkc† *family*	human homolog *PRKCA* as representative of RNA expression in tissue	Cordeiro *et al.* (2013)	14	3	6	7	4
Psma1	*C2, HC2, Pros-30*	Pihlajamäki *et al.* (2009)	79	66	85	83	98
Psmd12	*P55*	Pihlajamäki *et al.* (2009)	21	25	15	17	21
Rcan2	*Csp2, Dscr1l1, MCIP2, ZAKI-4*	Moeller *et al.* (2011)	32	4	16	8	32
Rxr† *family*	human homolog *RXRA* as representative of RNA expression in tissue	Cordeiro *et al.* (2013)	27	28	28	32	27
Slc16a4		Moeller *et al.* (2011)	113	12	11	3	12
Slc16a6		Lin *et al.* (2013)	1	1	2	5	2
Slc2a1	*Glut1*	Moeller *et al.* (2011)	13	2	4	11	9
Slc2a4	*Glut4*	Brunetto *et al.* (2012)	2	1	1	0	2
Sms	*SpmST*	Dong *et al.* (2009)	27	8	7	10	9
Snrpe		Pihlajamäki *et al.* (2009)	11	8	7	7	6
Srebf1†	*ADD-1, bHLHd1, SREBP1, SREBP-1a, SREBP1c*	Cordeiro *et al.* (2013)	27	63	51	26	31
Stc1		Moeller *et al.* (2011)	12	4	5	0	28
Tab1	*Map3k7ip1*	Puzianowska-Kuznicka *et al.* (2006)	9	6	10	13	8
Thra†	*Erba, Nr1a1, Rvr, Thra1, Thra2*	Ribeiro (2008)	27	3	27	13	25
Thrb†	*c-erbAbeta, Nr1a2, T3Rbeta, Thrb1, Thrb2*	Ribeiro (2008)	13	14	7	6	6
Thrsp	*S14, Spot 14*	Moeller *et al.* (2011)	2	143	0	0	5
Vldlr		Dong *et al.* (2009)	13	1	13	8	15

*according to Human Protein Atlas (http://www.proteinatlas.org; retrieved 2014-08-27)

†literature reference (analysis) on protein

FPKM, fragments per kilobase of exon per million fragments mapped

The table has been adapted from:

Langen B. (2015). Systemic effects after ionizing radiation exposure: Genome-wide transcriptional analysis of mouse normal tissues exposed to ^{211}At, ^{131}I, or 4 MV photon beam (Doctoral dissertation). Chalmers University of Technology, Gothenburg, Sweden (ISBN 978-91-7597-194-0).

The list is composed of data presented in:

Carreras MC, Peralta JG, Converso DP, Finocchietto PV, Rebagliati I, Zaninovich AA, Poderoso JJ. Modulation of liver mitochondrial NOS is implicated in thyroid-dependent regulation of O(2) uptake. *Am J Physiol Heart Circ Physiol*. 2001;281(6):H2282–8.

Chocron ES, Sayre NL, Holstein D, Saelim N, Ibdah JA, Dong LQ, Zhu X, Cheng SY, Lechleiter JD. The trifunctional protein mediates thyroid hormone receptor-dependent stimulation of mitochondria metabolism. *Mol Endocrinol*. 2012;26(7):1117–28.

Ribeiro MO. Effects of thyroid hormone analogs on lipid metabolism and thermogenesis. *Thyroid*. 2008;18(2):197–203.

Kim B. Thyroid hormone as a determinant of energy expenditure and the basal metabolic rate. *Thyroid*. 2008;18(2):141–4.

Cordeiro A, Souza LL, Einicker-Lamas M, Pazos-Moura CC. Non-classic thyroid hormone signalling involved in hepatic lipid metabolism. *J Endocrinol*. 2013 Jan 7. [Epub ahead of print]

Söderström M, Vo A, Heinzel T, Lavinsky RM, Yang WM, Seto E, Peterson DA, Rosenfeld MG, Glass CK. Differential effects of nuclear receptor corepressor (N-CoR) expression levels on retinoic acid receptor-mediated repression support the existence of dynamically regulated corepressor complexes. *Mol Endocrinol*. 1997;11(6):682–92.

Cheng SY, Leonard JL, Davis PJ. Molecular aspects of thyroid hormone actions. *Endocr Rev*. 2010;31(2):139–70.

Lin JZ, Sieglaff DH, Yuan C, Su J, Arumanayagam AS, Firouzbakht S, Cantu Pompa JJ, Reynolds FD, Zhou X, Cvoro A, Webb P. Gene specific actions of thyroid hormone receptor subtypes. *PLoS One*. 2013;8(1):e52407.

Moeller LC, Broecker-Preuss M. Transcriptional regulation by nonclassical action of thyroid hormone. *Thyroid Res*. 2011;4 Suppl 1:S6.

Brunetto EL, Teixeira Sda S, Giannocco G, Machado UF, Nunes MT. T3 rapidly increases SLC2A4 gene expression and GLUT4 trafficking to the plasma membrane in skeletal muscle of rat and improves glucose homeostasis. *Thyroid*. 2012;22(1):70–9.

Puzianowska-Kuznicka M, Pietrzak M, Turowska O, Nauman A. Thyroid hormones and their receptors in the regulation of cell proliferation. *Acta Biochim Pol*. 2006;53(4):641–50.

Pihlajamäki J, Boes T, Kim EY, Dearie F, Kim BW, Schroeder J, Mun E, Nasser I, Park PJ, Bianco AC, Goldfine AB, Patti ME. Thyroid hormone-related regulation of gene expression in human fatty liver. *J Clin Endocrinol Metab*. 2009;94(9):3521–9.

Dong H, Yauk CL, Rowan-Carroll A, You SH, Zoeller RT, Lambert I, Wade MG. Identification of thyroid hormone receptor binding sites and target genes using ChIP-on-chip in developing mouse cerebellum. *PLoS One*. 2009;4(2):e4610.

SUPPLEMENTAL TABLE 3. Significantly regulated ionizing radiation-associated genes

			Ionizing radiation (IR)-associated genes			
Mouse tissue	Time point	^{211}At activity	Gene symbol	Probe ID	Transcript ID	Fold change
Kidney cortex	1 h[b]	1.7 kBq	*Gadd45g*	ILMN_2903945	ILMN_222120	2.2
				ILMN_2744890	ILMN_222120	2.1
			Tnfrsf21	ILMN_2901626	ILMN_189811	2.0
				ILMN_2464573	ILMN_189811	1.9
	6 h[b]	1.7 kBq	*Gadd45g*	ILMN_2903945	ILMN_222120	1.9
				ILMN_2744890	ILMN_222120	1.8
Kidney medulla	1 h[b]	1.7 kBq	*Ccng1*	ILMN_2710229	ILMN_232357	-1.6
			Gadd45a	ILMN_2947568	ILMN_221926	-1.5
			Gja1	ILMN_1244291	ILMN_217762	1.6
			Tnfrsf21	ILMN_2901626	ILMN_189811	1.7
	6 h[b]	1.7 kBq	*Ccng1*	ILMN_2710229	ILMN_232357	-1.7
			Tnfrsf21	ILMN_2901626	ILMN_189811	1.7
	24 h[a]	1.8 kBq	*Ccng1*	ILMN_2710229	ILMN_232357	-1.8
			Fos	ILMN_2750515	ILMN_222500	1.5
			Gadd45g	ILMN_2903945	ILMN_222120	2.0
Liver	1 h[b]	1.7 kBq	*Tgfbr2*	ILMN_2760979	ILMN_221064	-1.5
			Trp53inp1	ILMN_2971479	ILMN_194391	1.9
				ILMN_2506012	ILMN_194391	1.7
			Trp53inp2	ILMN_2457585	ILMN_189011	1.8
	6 h[b]	1.7 kBq	*Trp53inp2*	ILMN_2457585	ILMN_189011	1.5
	24 h[a]	1.8 kBq	*Amy2*	ILMN_2874291	ILMN_234813	1.7
Lungs	1 h[b]	1.7 kBq	*Cdkn1a*	ILMN_2634083	ILMN_209664	1.9
			Trp53inp1	ILMN_2971479	ILMN_194391	2.1
Spleen	1 h[b]	1.7 kBq	*Trp53inp1*	ILMN_2971479	ILMN_194391	2.0
	24 h[a]	1.8 kBq	*Amy2*	ILMN_2874291	ILMN_234813	133
			Pcna	ILMN_2762026	ILMN_223289	-1.6
	7 d[b]	1.7 kBq	*Amy2*	ILMN_2874291	ILMN_234813	5.0

Analysis performed on microarray data [a]GEO:GSE40806 and [b]GEO:GSE56894 first reported in Langen *et al.* (2013) and Langen *et al.* (2015), respectively. ID, identification number

SUPPLEMENTAL TABLE 4. Significantly regulated thyroid hormone-responding genes

			Thyroid hormone-responding genes			
Mouse tissue	Time point	^{211}At activity	Gene symbol	Probe ID	Transcript ID	Fold change
Kidney cortex	1 h[b]	1.7 kBq	*G6pc*	ILMN_1245103	ILMN_219085	2.4
			Pck1	ILMN_1213632	ILMN_238641	1.8
	6 h[b]	1.7 kBq	*G6pc*	ILMN_1245103	ILMN_219085	1.9
			Pck1	ILMN_1213632	ILMN_238641	3.4
	24 h[a]	1.8 kBq	*Pfkp*	ILMN_1237695	ILMN_226308	1.8
	7 d[b]	1.7 kBq	*G6pc*	ILMN_1245103	ILMN_219085	1.6
			Thrsp	ILMN_1256775	ILMN_209127	-2.9
Kidney medulla	1 h[b]	1.7 kBq	*G6pc*	ILMN_1245103	ILMN_219085	2.3
			Pck1	ILMN_1213632	ILMN_238641	3.3
			Pfkp	ILMN_1237695	ILMN_226308	-1.9
	6 h[b]	1.7 kBq	*G6pc*	ILMN_1245103	ILMN_219085	2.6
			Pck1	ILMN_1213632	ILMN_238641	2.8
			Pfkp	ILMN_1237695	ILMN_226308	-1.7
	24 h[a]	1.8 kBq	*Fos*	ILMN_2750515	ILMN_222500	1.5
			Slc16a4	ILMN_2856537	ILMN_222374	-2.8
Liver	1 h[b]	1.7 kBq	*Cyp7a1*	ILMN_2604383	ILMN_210317	2.6
			Egfr	ILMN_2693922	ILMN_211300	2.0
			G6pc	ILMN_1245103	ILMN_219085	2.6
			Lmo2	ILMN_2767605	ILMN_223680	-1.6
			Pck1	ILMN_1213632	ILMN_238641	2.2
			Thrsp	ILMN_1256775	ILMN_209127	3.8
	6 h[b]	1.7 kBq	*Cyp7a1*	ILMN_2604383	ILMN_210317	2.6
			G6pc	ILMN_1245103	ILMN_219085	2.3
			Pck1	ILMN_1213632	ILMN_238641	2.3
			Thrsp	ILMN_1256775	ILMN_209127	3.9
	24 h[a]	1.8 kBq	*Egfr*	ILMN_3052260	ILMN_207468	-1.8
				ILMN_3128725	ILMN_207468	-1.8
			Srebf1	ILMN_2792089	ILMN_218526	-1.9
			Thrsp	ILMN_1256775	ILMN_209127	-1.9
	7 d[b]	1.7 kBq	*Cyp7a1*	ILMN_2604383	ILMN_210317	1.8
			G6pc	ILMN_1245103	ILMN_219085	2.3
Lungs	1 h[b]	1.7 kBq	*Cdkn1a*	ILMN_2634083	ILMN_209664	1.9
	24 h[a]	1.8 kBq	*Myh6*	ILMN_2788836	ILMN_259107	-1.7
			Thrsp	ILMN_1256775	ILMN_209127	1.6
Spleen			*none present*			

Analysis performed on microarray data [a]GEO:GSE40806 and [b]GEO:GSE56894 first reported in Langen *et al.* (2013) and Langen *et al.* (2015), respectively. ID, identification number